

UKAEA-CCFE-PR(18)67

Jonathan Shimwell, Remi Delaporte-Mathurin, Jean-Charles Jaboulay, Julien Aubert, Chris Richardson, Chris Bowman, Andrew Davis, Jamie Bernardi, Sikander Yasin, Xiaoying Tang

# **Multiphysics analysis with CAD based parametric breeding blanket creation for rapid design iteration**

Enquiries about copyright and reproduction should in the first instance be addressed to the  
UKAEA

Publications Officer, Culham Science Centre, Building K1/O/83 Abingdon, Oxfordshire,  
OX14 3DB, UK. The United Kingdom Atomic Energy Authority is the copyright holder.

# **Multiphysics analysis with CAD based parametric breeding blanket creation for rapid design iteration**

Jonathan Shimwell, Remi Delaporte-Mathurin, Jean-Charles Jaboulay, Julien Aubert , Chris Richardson, Chris Bowman, Andrew Davis, Jamie Bernardi, Sikander Yasin, Xiaoying Tang



# CAD based parametric breeding blanket creation for rapid design iteration

Jonathan Shimwell<sup>1</sup>, Rémi Delaporte-Mathurin<sup>2</sup>, Jean-Charles Jaboulay<sup>3</sup>, Julien Aubert<sup>3</sup>, Chris Richardson<sup>4</sup>, Chris Bowman<sup>5</sup>, Andrew Davis<sup>1</sup>,  
Jamie Bernardi<sup>6</sup>, Sikander Yasin<sup>8</sup>, Xiaoying Tang<sup>9</sup>

<sup>1</sup>Culham Centre for Fusion Energy (CCFE), Culham Science Centre, Abingdon, Oxfordshire, OX14 3DB, UK

<sup>2</sup>Département Thermique-Énergétique, Polytech Nantes, Université de Nantes, rue Christian Pauc CS 50609, 44306 Nantes Cedex 3, France

<sup>3</sup>Den-Département de modélisation des systèmes et structures (DM2S), CEA, Université Paris-Saclay, F-91191 Gif-sur-Yvette, France

<sup>4</sup>BP Institute, Bullard Laboratories, Madingley Road, Cambridge CB3 0EZ, UK

<sup>5</sup>York Plasma Institute, University of York, Heslington, YO10 5DD, UK

<sup>6</sup>University of Cambridge, The Old Schools, Trinity Ln, Cambridge CB2 1TN, UK

<sup>7</sup>University of Manchester, Oxford Rd, Manchester, M13 9PL, UK

<sup>8</sup>School of Mechanical Engineering, Shanghai Jiao Tong University, Shanghai 200240, China

---

## Abstract

Breeding blankets are designed to ensure tritium self-sufficiency in deuterium-tritium fusion power plants. In addition to this, breeder blankets play a vital role in shielding key components of the reactor, and provide the main source of heat which will ultimately be used to generate electricity. The design of blankets is critical to the success of fusion reactors and integral to the design process. Neutronic simulations of breeder blankets are regularly performed to ascertain the performance of a particular design. An iterative process of design improvements and parametric studies are required to optimise the design and meet performance targets. Within the EU DEMO program the breeding blanket design cycle is repeated for each new baseline design. One of the key steps is to create 3D models suitable primarily for use in neutronics, but could be used in other CAD based physics and engineering analysis. This article presents a novel blanket design tool which automates the process of producing heterogeneous 3D CAD based geometries of the Helium Cooled Pebble Bed, Water Cooled Lithium Lead, Helium Cooled Lithium Lead, and the Dual Cooled Lithium Lead. The blanket design tool described in this paper provides parametric geometry for use in neutronics and engineering simulations. This paper explains the methodology of the design tool and demonstrates use of the design tool by generating all four EU blanket designs using the EU DEMO baseline. Neutronics and heat transfer simulations using the models have been carried out. The approach described has the potential to considerably speed up the design cycle and greatly facilitate the integration of multiphysics studies.

**Keywords:** Fusion, parametric, CAD, neutronics, 3D, model, breeder, blanket, engineering

---

## 1. Introduction

Breeding blankets are designed to fulfill several high level plant requirements including: tritium self sufficiency, shielding non sacrificial components from the intense neutron flux, and producing heat which is ultimately used to generate electricity. Designing and engineering components for use within fusion reactors is challenging due to the high radiation fluxes and significant heat loads that they experience. Maintaining an operational and safe component within the inner vessel of a fusion reactor presents a range of difficulties, however adding functional requirements such as tritium breeding, heat generation and heat removal further complicates the task.

Methods of design optimisation such as parameter studies and “designing by analysis” approach are possible avenues for designing fusion reactor components that could provide solutions to this challenge. Such methods rely on human intuition and iterative analysis of models to close in on an optimal solutions. Performing analysis in an isolated discipline will only find the optimal solution for performance metrics that are obtainable within that discipline. For instance neutronics optimisations may find the tritium breeding ratio (TBR) but may find unacceptable temperatures. Multi-physics analysis is required to optimise component design. To maintain data provenance it would be preferable to have a single model basis when sharing data between analysis techniques.

Traditionally models are generated for neutronics using constructive solid geometry (CSG) and the models are suitable to be used in parametric studies. Engineering analysis tends to require CAD models and CSG models are typically not compatible with Engineering programs. Models for use in engineering analysis are often created via graphical user interfaces. The process of creating new engineering and neutronics models can be a time consuming exercise. This is compounded since the models must be generated with the release of a new EU DEMO baseline design, and there also being four EU blanket designs for each iteration.

To analyse the performance of different designs within the parameter space it would be desirable to have an accurate 3D geometry produced rapidly. Adopting a common geometry format would allow geometry to be used in multiple domains. Allowing fine details (such as cooling pipes) to be included or excluded during the model generation can facilitate specific requirements of the particular analysis. Use of open source geometry producing software such as FreeCAD [1], Salome [2] or PythonOCC [3] can be used to quickly generate parametric CAD geometry which can be exported into a variety of formats. CAD files in STEP format [4] are an open file standard compatible with engineering simulation software. STEP files can be easily converted into surface faceted geometry (e.g. h5m or STL files) for use in neutronics codes such as DAG-MCNP5/6 [5] and Serpent 2 [6]. Ideally any solution to making component models would be flexible enough to work with new DEMO baseline models and also to produce different blanket designs.

## 2. Method

### 2.1. Geometry creation

It is clear that in order for any advanced method to generate any detailed geometry it must require the minimum human intervention, it was determined that a software library should be created that allows arbitrary geometric operations to be performed, with the end goal of creating parametrically built blanket modules for the EU Demo program. This software is called the “Breeder Blanket Model Maker” and can be found here [7]. Routines for the generation, modification and serialisation of blanket envelopes were created that ultimately automatically produce detailed heterogeneous blankets for use in DEMO modelling. Demonstration neutronic and heat diffusion simulations were performed to demonstrate the ease of carrying out parameter studies. Parametric models of all four EU blanket designs for single-module segments were generated to demonstrate the design tool. These include the Helium Cooled Pebble Bed Blanket (HCPB) [8], Helium Cooled Lithium Lead Blanket (HCLL) [9], Water Cooled Lithium Lead Blanket (WCLL) [10] and Dual Coolant Lithium Lead Blanket (DCLL) [11]. The process has been broken down into two parts, the first flowchart (see Figure 1) summarises the construction of all the non breeder zone components, this includes the first wall, armour, and rear plates. The second flowchart (see Figure 2) summaries the construction of the breeder zone structure.

The EU DEMO baseline model [12] has 26 different blanket modules which have different shapes, orientations, and positions depending upon the positioning within the reactor (see stage 1 in Figure 1). The blanket designs share some common features such as: filleted corners on the toroidal HCPB, HCLL and WCLL designs or poloidal DCLL edges.

#### *Structural Components*

The procedure for the creation of the structural part of the blanket module is performed first the following stage generates internal detail of the breeder zone. A number of key parameters define the structure of the blanket; first wall armour thickness, first wall thickness, rear plate count & thickness and end cap thickness. An automated procedure regarding the automatic construction of a full detailed blanket structure was defined, where the full implementation details can be found in [7]. Additional fine detail is also included at the users discretion including the introduction of fillets and cooling channels. The overall programmatic flow is shown in Figure 2, where differing blankets follow different logical routes.

#### *Breeder zone components*

In order to generate the full heterogeneous blanket description the internal detail of the breeder zone must be generated. This is a two stage process where first the cooling structure is generated starting from the breeder zone envelope and generating the cooling structure from it. The last stage is to subtract the cooling structure from the breeder zone envelope, leaving the non-structural breeding material (LiPb/Lithium Ceramic/Neutron Multiplier).

#### *Cooling Structure Generation*

The segmentation of the cooling structure varies for each of the four breeder blanket modules, but is almost entirely a combination of poloidal, toroidal and radial based segmentations. The cooling structure of the HCLL advanced plus module [9] can be represented by a series of poloidal segmentations with alternating layers of cooling plates. This can be reproduced using alternate poloidal segmentation with alternating poloidal extrusion lengths as shown in Figure 2 section 2. In the case of the HCPB module there are alternating poloidal layers of lithium ceramic and neutron multiplier between the cooling plates. The poloidal segmentation functions have been designed to allow any number of layer repetition, this is demonstrated in stage 3 of Figure 2). The wedge shaped regions at the upper and lower extremities of the HCPB module are filled with neutron multiplier and are therefore not considered part of the cooling structure. The software is able to identify these wedge shaped regions and group them with the other neutron multiplier regions.

Radial cuts and thereby radial segmentation is also implemented, these are required for both the WCLL and the DCLL blanket designs. The WCLL cooling structure can be generated with a combination of poloidal and toroidal segmentation (see stage 6 in Figure 2). Both the toroidal and poloidal directions have alternating thicknesses for the structural plates and the lithium lead regions. Every other layer of poloidal structural plate has an offset from the first wall, that allows lithium lead to flow between plates. The poloidal segmentation for such a model can be carried out

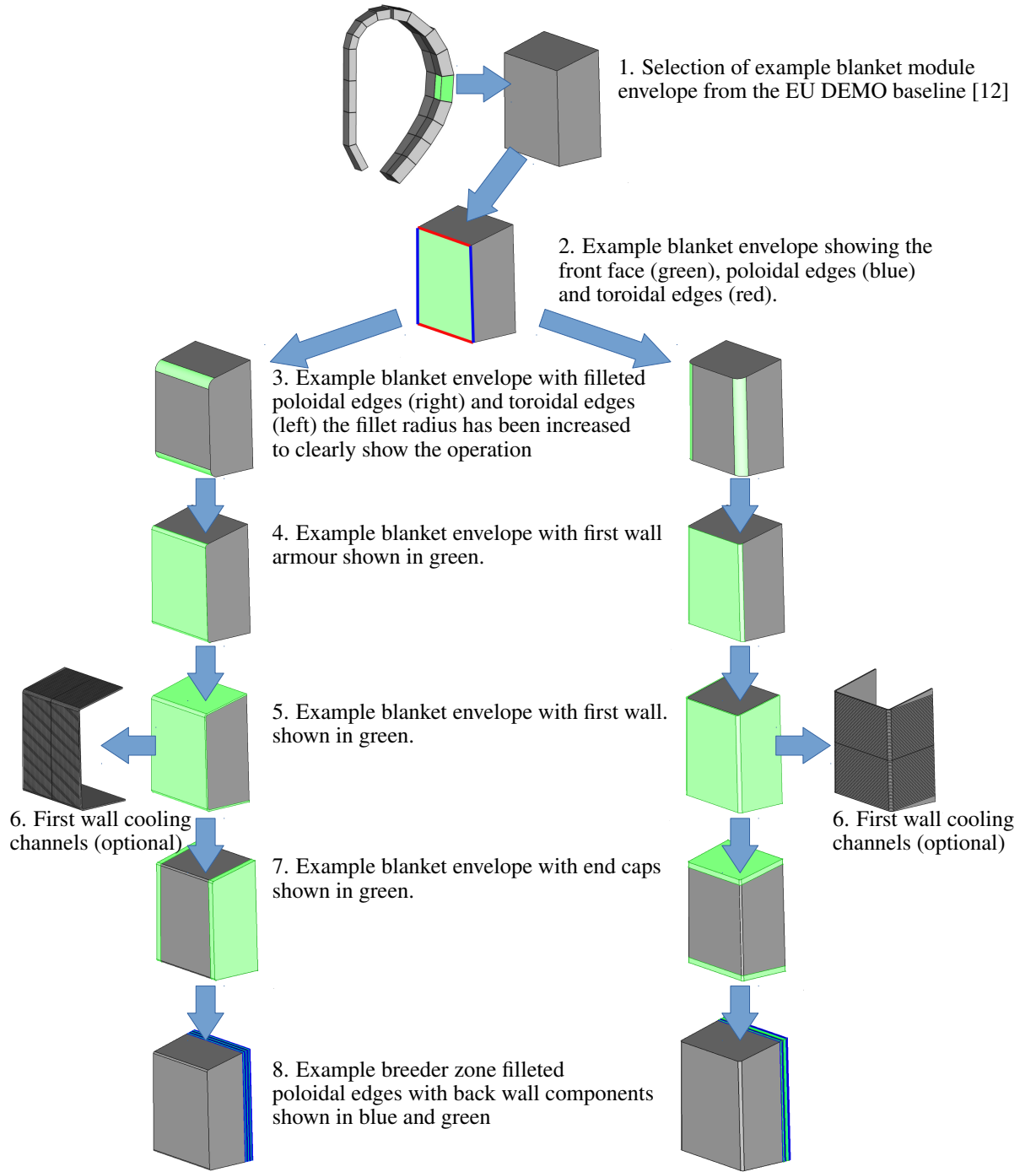


Figure 1: Automated workflow for generating first wall, end caps and back plates from EU DEMO baseline [12] blanket envelopes.

in a similar way to the HCLL, however the WCLL has an additional complication which requires radial segmentation. The WCLL model requires toroidal segmentation and additionally requires that the upper and lower wedge volumes should be considered to be entirely lithium lead. The resulting product of the toroidal segmentation can be seen in



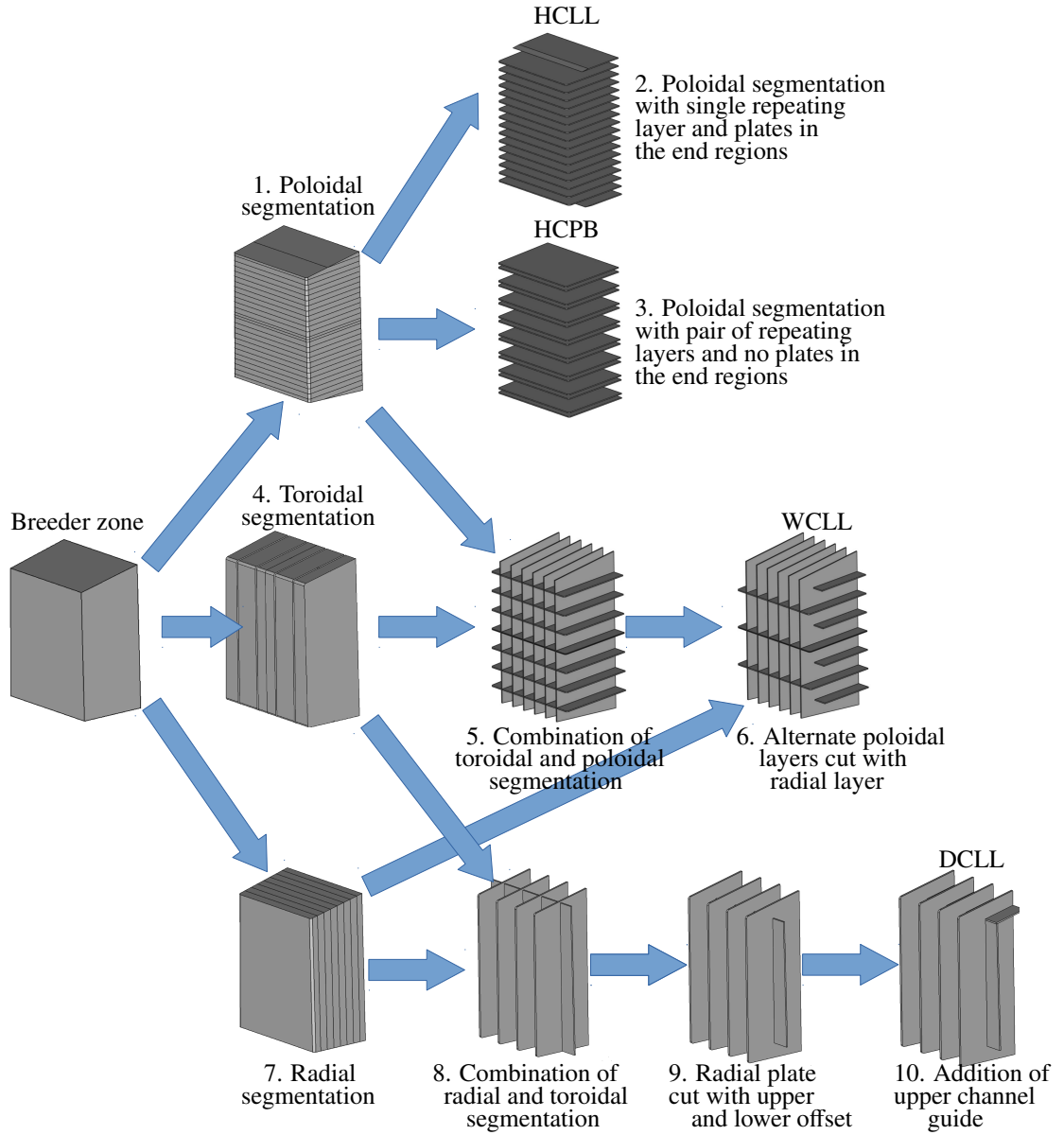


Figure 2: Creation of internal breeder zone structure using a combination of toroidal, poloidal and radial segmentations

stage 6 in Figure 2).

The DCLL cooling structure can be formed from a combination of radial and toroidal segmentation plus some detail to guide the flow of lithium lead. The procedure used was to first radially segment the blankets into three or five parts (depending upon the radial depth of the blanket). In general most of the inboard blankets accommodate three radial layers and the outboard blankets accommodate five radial layers. The addition of toroidal segmentation to the previously radial segmented breeder zone forms the first stage of the DCLL model (see stage 8 of Figure 2). The DCLL blanket design allows the lithium lead to flow around the structure. An additional structural component at the upper end of each blanket module is also required by the DCLL design, the only additional complication is that a Boolean subtraction with the first radial layer is also required to obtain the desired structural plate shape (see stage 10 of Figure 2).

### *Breeding Material*

The complete description of the breeder zone is the cooling structure description and the description of the breeding material. The final stage is take the original breeder zone envelope and subtract the newly created cooling plants from it, thus defining the complete breeding zone description. In the cases of the HCLL, WCLL and DCLL all require that the end caps are lithium lead and HCPB required the end caps to be neutron multiplier.

## 2.2. Parametric geometries

As a result of the method previously described there is now an automated procedure for obtaining semi detailed CAD geometry for the HCPB, HCLL, WCLL and DCLL blankets. The process relies on a library of common functions which can be mixed and matched to create particular blanket designs. The breeder blanket design tool is released as an open source project under the Apache 2.0 license and is distributed via the UKAEA Github repository [7]. The software is subject to a test suite and the build status is updated automatically with every commit. Continuous integration practices are employed using Circle CI and Docker.

The model construction process is parametric which allows models required for parameter studies to be generated rapidly. Currently the parameters that a user can input are:

- filename of blanket envelope required for segmentation
- blanket type (HCPB, HCLL, WCLL, DCLL)
- poloidal fillet radius for first wall and first wall armour
- toroidal fillet radius for first wall and first wall armour
- first wall armour thickness
- first wall thickness
- end cap thickness
- thickness of each rear plate
- thickness of each poloidal segmentation
- thickness of each toroidal segmentation
- thickness of each radial segmentation
- first wall coolant channel poloidal height
- first wall coolant channel radial height
- first wall coolant channel pitch
- first wall coolant channel offset from the front face
- output file format (STEP or STL) and tolerance.

Not all parameters are needed for each design as some are not applicable, for instance the breeder zone in the HCPB blanket has no radial segmentation option and does not require this input. The following Figures show each of the four blanket designs formed from a particular module from the baseline DEMO model [12]. The process of building a blanket module from an envelope is typically a few seconds on a single core. Build time depends on the input parameters as many very small layers would necessitate more Boolean operations than for the case of a few large layers. The process is parallelisable and therefore a model such as the EU DEMO with 26 blanket modules typically takes less than 5 minutes on a quad core Intel i5 7600 CPU.

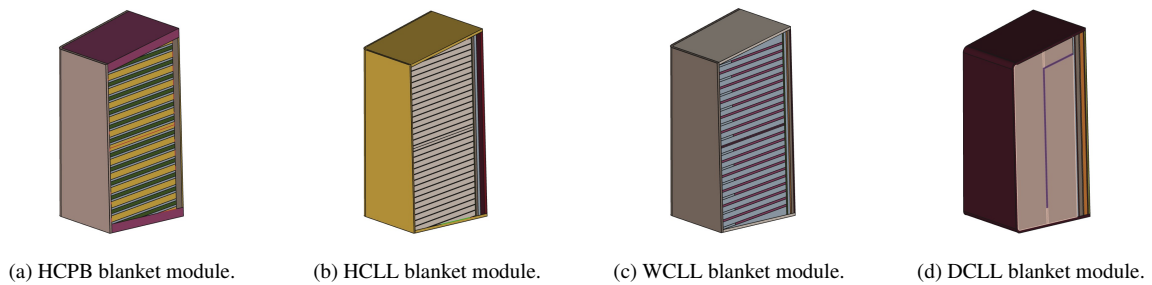


Figure 3: Example parametric blanket modules, parameter values have been enlarged in some cases to increase visibility of components

### 3. Results

#### 3.1. Neutronics model creation

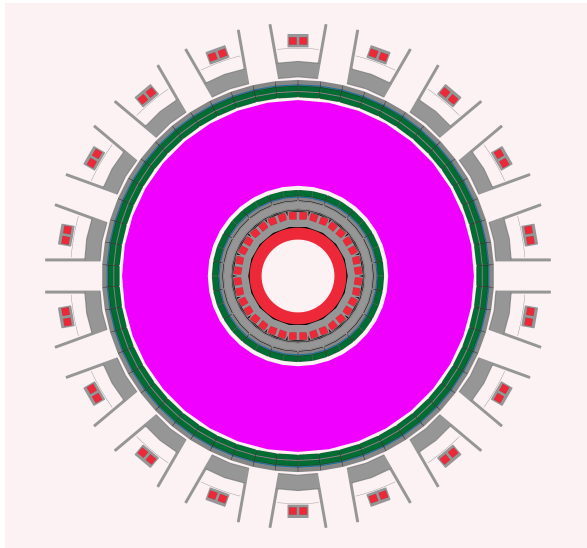
Once the parametric CAD models have been created one potential use case is neutronics simulations. There are several routes from CAD to neutronics models such as conversion to constructive solid geometry using conversion software such as McCad [13] or SuperMC [14]). Alternatively use of faceted geometry is also possible. Previously parameter studies for fusion blanket optimisation have converted parametric CAD models to CSG models using McCad and performed the simulation using MCNP [15]. This study opted to simulate using faceted geometry in the STL file format and perform the neutronics simulation using Serpent 2, which natively supports STL geometry. The process of converting from STEP to STL is quicker than STEP to CSG and the results are easier to visually verify. To demonstrate practical use of the parametric geometry, a series of tritium breeding simulations were obtained for the HCLL. The poloidal height of the lithium lead sections and the  ${}^6\text{Li}$  enrichment of the lithium lead were varied independently. The thickness of the first wall and the cooling plates were varied simultaneously with the poloidal height of the lithium lead sections using Equations 1 and 2.

$$FWT = C_D + \sqrt{\frac{C_p \times LL_p^2}{4 \times SmD}} = 0.01 + 9.552 \times 10^{-2} \times LL_p \quad (1)$$

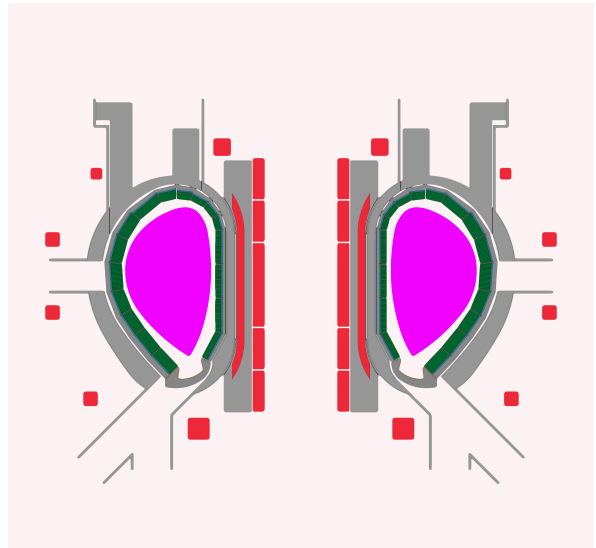
$$CPT = \frac{C_p \times LL_p}{1.1 \times SmD} = 3.332 \times LL_p \quad (2)$$

Where FWT is the firstwall thickness (m), CPT is the cooling plate thickness (m),  $C_D$  is the radial diameter of the first wall cooling channel (0.01 m),  $C_p$  is the coolant pressure (10 MPa), SmD is the stress limit criteria for Eurofer (274 MPa) and  $LL_p$  (m) is the poloidal height of the lithium lead sections. The equations are described in more detailed in [16] and [17]. This HCLL study is a demonstration of the model making tool developed, thermal-mechanical constraints are not taken into account.

Halton sampling [18] was used as the sampling technique to select points within the parameter space. The parameter space encompassed blankets with a poloidal height of the lithium lead between 0.01 m and 0.12 m and  ${}^6\text{Li}$  enrichment between 0 and 100%. FENDL 3.1b [19] cross sections were used for neutron transport. Neutronics materials definitions from the Eurofusion material composition [20] were used in the model and a parametric plasma source based on [21] with plasma parameters from [22] was used. The number of starting particles (NPS) run for each TBR simulation was  $1 \times 10^7$ .



(a) Slice of EU Demo viewed from above



(b) Slice of EU Demo side view.

Figure 4: A neutronics model of EU Demo using faceted geometry (STL) with detailed HCLL blankets. Showing plasma ■, lithium lead ■, magnets ■, tungsten ■ and structural steels ■.

### 3.2. Neutronics simulations

The models generated are suitable for neutronics simulations and Figure 5 shows the resulting TBR values from a neutronics parameter study. TBR was found to change with the poloidal height of lithium lead. Models with small poloidal height contain a relatively large Eurofer fraction due to the large number of cooling plates, this appears to have reduced the tritium production. However models with large poloidal height can also have large quantities of Eurofer in the breeder blanket. As the poloidal lithium lead height increase the thickness of the Eurofer first wall also increases (see Equation 1) and the thickness of the Eurofer cooling plates also increases (see Equation 2).

There appears to be an optimal poloidal height which becomes more pronounced with  $^6\text{Li}$  enrichment. Figure 5 shows the variation of TBR with  $^6\text{Li}$  atom fraction within the lithium lead. Increasing  $^6\text{Li}$  enrichment shows an increase in TBR as confirmed by previous studies [23]. Figure 5 shows the variation of TBR with the poloidal height of the lithium lead regions within the breeder zone of the blanket. The poloidal height has less of an effect of TBR but can be optimised increase TBR by nearly 0.1. at 90%  $^6\text{Li}$  enrichment. Figure 5 shows that each different enrichment of  $^6\text{Li}$  has a different optimal height for the poloidal lithium lead. The size of the  $5\sigma$  confidence regions varies depending on the proximity and statistical error of nearby simulations. This is most noticeable towards the extremities of the search space where there are less simulations and the size of the  $5\sigma$  confidence regions is larger.

A maximum TBR of  $1.278 \pm 0.010$  ( $5\sigma$  confidence) was found using Gaussian process software [24] to fit the simulation data and statistical error (see Figure 5). The highest TBR value was found for a blanket design with a lithium lead poloidal height of 0.061 m and a  $^6\text{Li}$  enrichment of 100%.

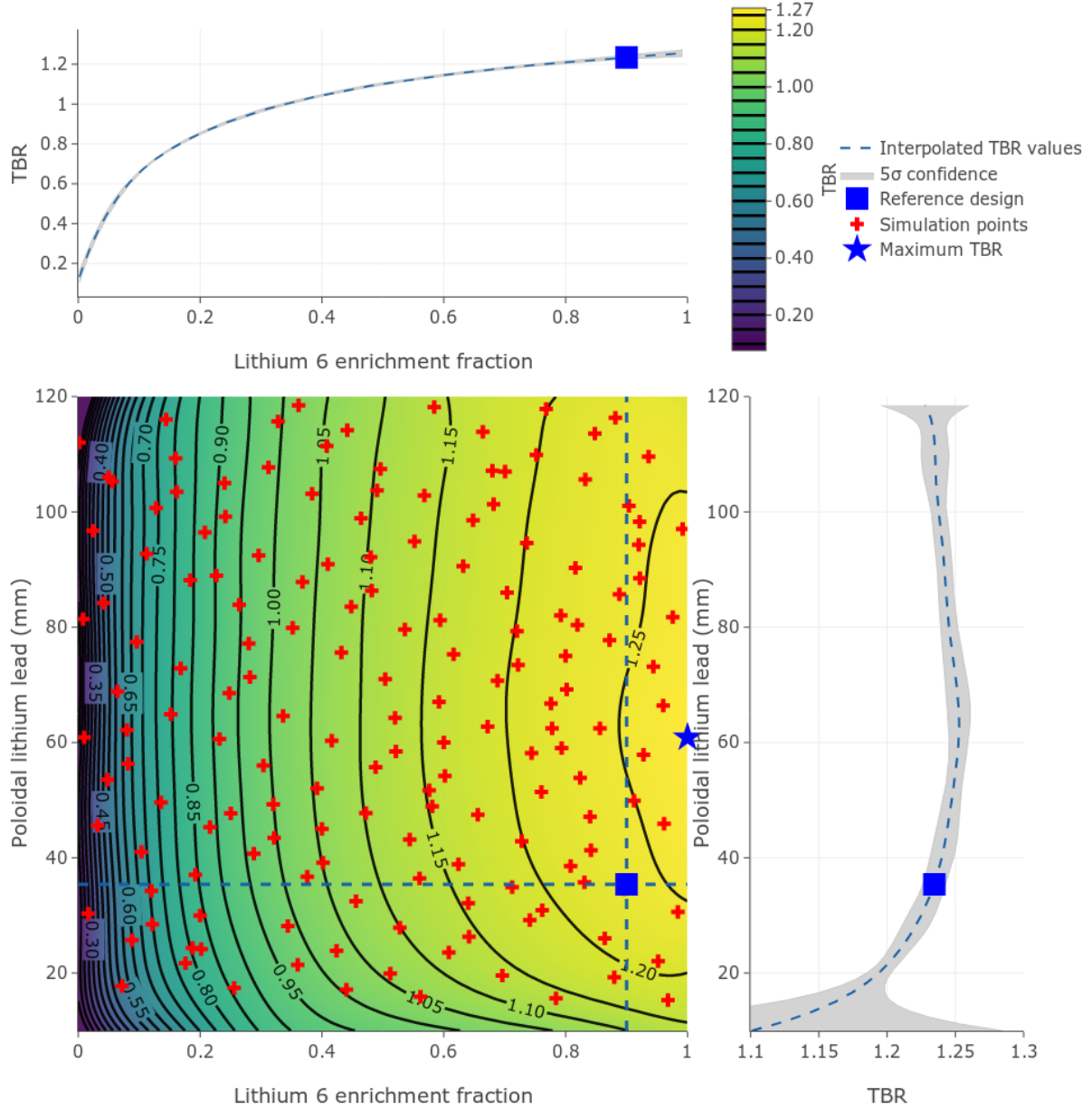


Figure 5: Showing interpolated TBR values with a  $5\sigma$  confidence for a range of different  $^6\text{Li}$  enrichments and poloidal lithium lead height. The Gaussian process software used [24] was able to fit the TBR values along with their statistical errors and find the confidence values. The reference design HCLL has 90%  $^6\text{Li}$  enrichment, 34.5mm of poloidal lithium lead and achieves a TBR of 1.235.

### 3.3. Heat diffusion model creation

A slice of the HCLL blanket geometry was used to create a simplified model of the temperature field in the tungsten, EUROfer and lithium lead. A tetrahedral mesh was created using Trellis [25] complete with surface and volume boundary conditions. Heat diffusion simulations were carried out using FEniCS [26] which was able to apply boundary conditions to surfaces and temperature dependent materials properties to different volumes. The heat diffusion equation used is described by Equation 3.

$$\nabla^2(\lambda T) + Q = 0 \quad (3)$$

Where  $T$  is the temperature in K,  $\lambda$  the thermal conductivity of the given material expressed in  $\text{W m}^{-1} \text{K}^{-1}$  and  $Q$  the volumetric source term in  $\text{W m}^{-3}$ . As this equation is solved using the Finite Elements Method (FEM), Equation 3 needs to be brought to its weak formulation (or variational formulation) as follows:

$$\lambda \left( \int_{\partial\Omega} \frac{\delta T}{\delta n} v dS - \int_{\Omega} \nabla v \nabla T dx \right) = \int_{\Omega} v Q dx \quad (4)$$

$$\Omega \in \mathbb{R}^3$$

Where  $\Omega$  is the domain on which Equation 4 is solved,  $n$  is the normal direction on the external surface and  $v$  is a test function. The integration term on the boundary of  $\Omega$  is determined by the boundary conditions.

Two types of boundary conditions are used in this model:

- Robin boundary conditions:

The Robin boundary condition allows the assignment of a convective heat flux on a boundary. In Equations 5 and 6, it is shown that the heat flux depends on the temperature of the fluid and the convective coefficient  $h$  in  $\text{W m}^{-2} \text{K}^{-1}$ . This coefficient depends on the type of convection (natural, forced, laminar or turbulent) and the fluid in contact with the surface.

$$-\lambda \frac{dT}{dn} = h_{FWCC}(T - T_{FWCC}) \quad \text{on } \Gamma_{FWCC} \quad (5)$$

$$-\lambda \frac{dT}{dn} = h_{HSPCC}(T - T_{HSPCC}) \quad \text{on } \Gamma_{HSPCC} \quad (6)$$

$\Gamma_{FWCC}$  and  $\Gamma_{HSPCC}$  are surface domains respectively and are shown in blue and purple in Figure 6. This condition is used on the surfaces of the helium cooling channels. The coefficients  $h$  have been calculated for the First Wall Cooling Channels (FWCC) and Horizontal Stiffening Plate Cooling Channels (HSPCC). They are determined using Gnielinski correlation (Equation 7) with the parameters in Table 1 in accordance with [16].

$$Nu_D = \frac{h D_h}{\lambda_{He}} = \frac{(\xi/8)(Re_D - 1000)Pr}{1 + 12.7(\xi/8)^{1/2}(Pr^{2/3} - 1)} \quad (7)$$

Where  $Nu_D$  is the Nusselt number,  $D_h$  is the hydraulic diameter in m,  $\lambda_{He}$  is the thermal conductivity of the fluid in  $\text{W m}^{-1} \text{K}^{-1}$ ,  $Re_D$  is the Reynolds number and  $Pr$  is the Prandtl number. We consider a smooth surface and thereby the Darcy-Weisbach friction factor  $\xi$  is then given by:

$$\xi = (0.790 \ln Re_D - 1.64)^{-2}$$

- Neumann boundary conditions:

By using Neumann boundary conditions, fixed heat flux can be assigned to the front wall armour surface shown in red in Figure 6 as described in Equation 8.

$$-\lambda \frac{\delta T}{\delta n} = J \quad \text{on } \Gamma_{FW} \quad (8)$$



Symbol	Description	Value FW CC	Value HSP CC
$Re_D$	Reynolds number	$1.310 \times 10^5$	$3.018 \times 10^4$
$Pr$	Prandtl number	$6.599 \times 10^{-1}$	$6.599 \times 10^{-1}$
$\xi$	Darcy-Weisbach friction factor	$3.000 \times 10^{-2}$	$2.000 \times 10^{-2}$
$D_h$	Hydraulic diameter (m)	$1.500 \times 10^{-2}$	$3.000 \times 10^{-3}$
$h$	Convective coefficient ( $\text{W m}^{-2} \text{K}^{-1}$ )	$4.531 \times 10^3$	$4.848 \times 10^3$
$T_{coolant}$	Temperature of coolant (K)	$7.232 \times 10^2$	$6.232 \times 10^2$

Table 1: Parameters used for the determination of the convective coefficients  $h_{FWCC}$  and  $h_{HSPCC}$

Here,  $J$  yields for a fixed flux density in  $\text{W m}^{-2}$  on a boundary. This condition is used on the surface  $\Gamma_{FW}$  which corresponds to the front wall (shown in red in Figure 6) with a flux of  $J = 0.5 \text{ MW m}^{-2}$  which corresponds to the heat flux emitted by the plasma.

The rest of the surfaces (shown in grey in Figure 6) are considered as insulated. This assumption is valid as long as these surfaces are part of a vacuum and are not exposed to intense heat flux. The values of the thermal conductivity  $\lambda$  in  $\text{W m}^{-1} \text{K}^{-1}$  in Equation 4 were found in [27].

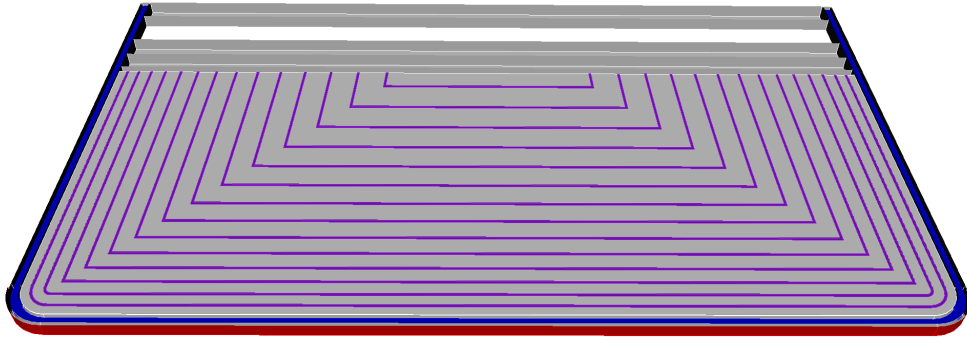


Figure 6: Cut of a HCLL module slice showing surfaces used for boundary conditions.  $\Gamma_{FW}$  (red),  $\Gamma_{FWCC}$  (blue) and  $\Gamma_{HSPCC}$  (purple).

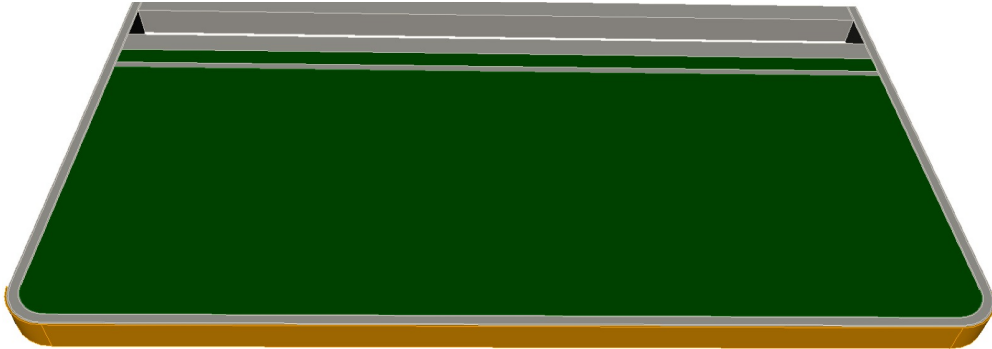


Figure 7: HCLL module slice showing materials. Tungsten (orange), LiPb (green) and Eurofer (grey).

Finally, the distribution of the volumetric source term  $Q$  in Equations 3 and 4 is given by [28]. The spatial distribution of  $Q$  is shown in Figure 8.

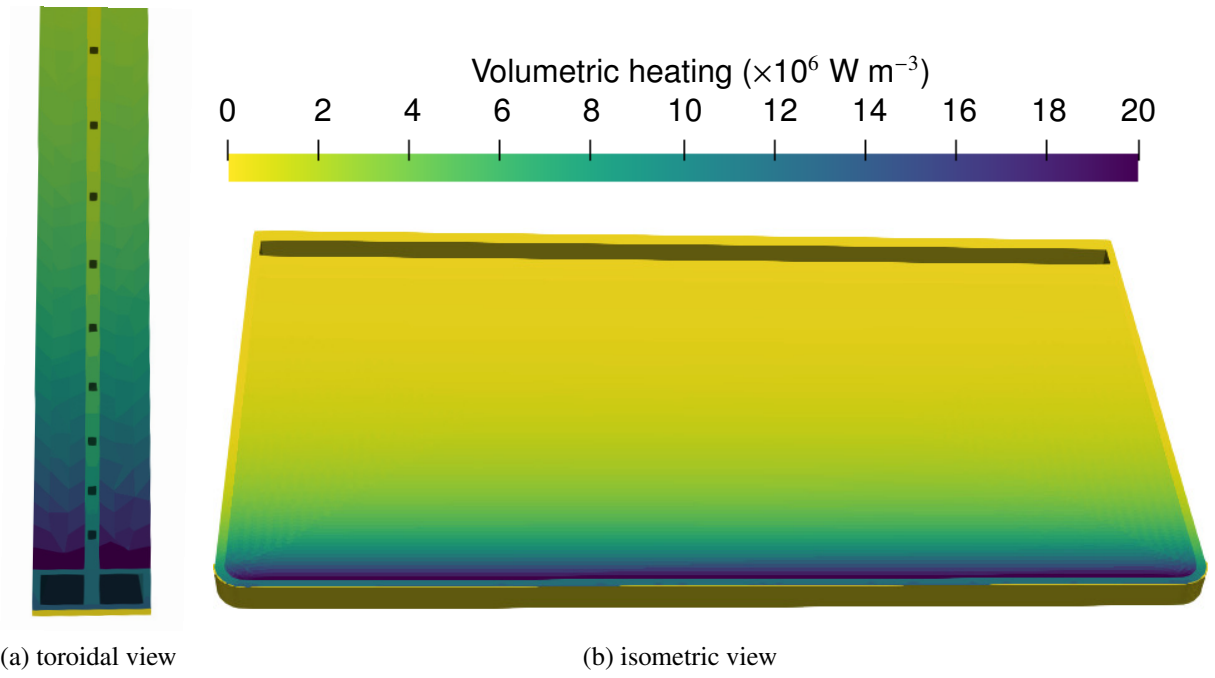


Figure 8: Volumetric heating source term applied to a slice from middle of the equatorial outboard blanket module in  $\text{Wm}_{-3}$ .

### 3.4. Heat diffusion simulations

Using the same generated models as in Section 3.2, heat diffusion simulations have been performed. The steady state solution of the temperature field is shown in Figure 9. Thanks to these simulations, we are able to determine the maximum temperature reached by each material and determine if the design allows the materials to stay within their maximum operation temperature limits (550°C for Eurofer and 1300°C for tungsten [29]). The maximum temperatures are shown in Table 2.

Material	Maximum temperature (K)	Maximum temperature (°C)
Tungsten	816	543
Lithium lead	859	586
EUROfer	808	535

Table 2: Maximum temperatures of each material

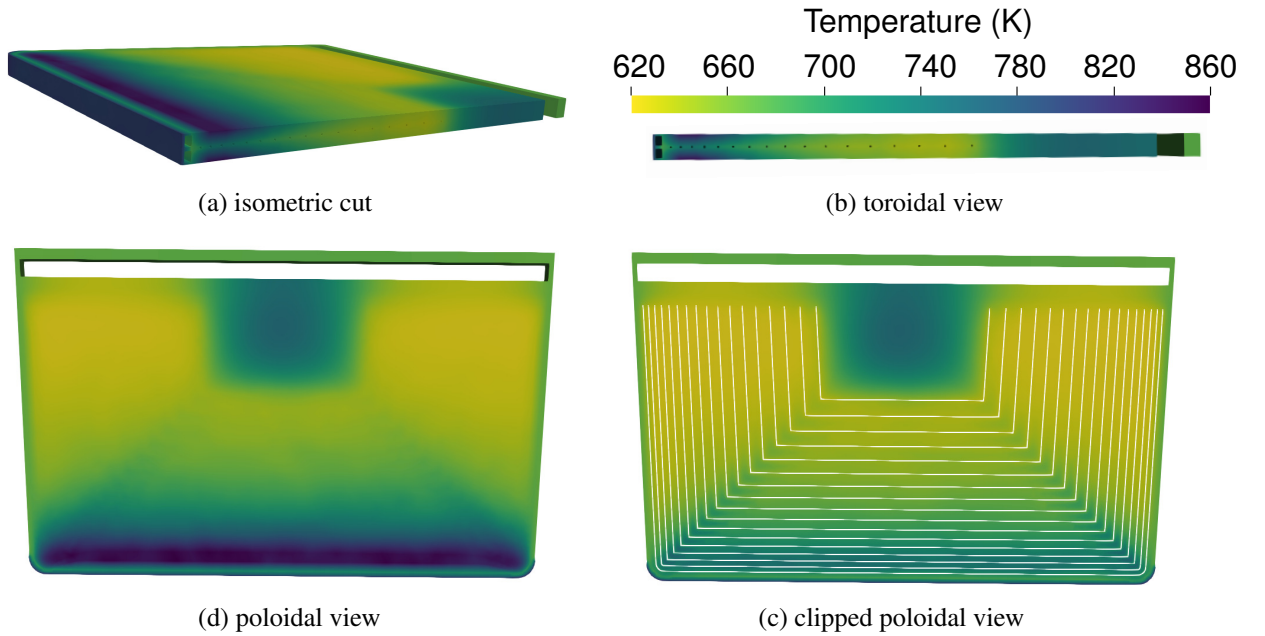


Figure 9: Resulting temperature field of a slice from middle of the equatorial outboard blanket module in K.

#### 4. Conclusion

A design tool capable of generating parametric designs for fusion breeder blankets has been demonstrated on single module blanket envelopes for the HCLL, HCPB, WCLL and DCLL. A wide range of design parameters can be changed to generate CAD geometry for use in parameter studies. The geometry generated is available in CAD format (STEP) and faceted geometry (STL and h5m). Conversion to CSG for neutronics simulation can be achievable via existing software such as McCad or MCAM. Although the option of faceted geometry allows CSG geometry to be avoided in favor of more CAD based neutronic simulation techniques such as DAGMC or Serpent 2. The provision of CAD geometry also enables manipulation to be performed with standard CAD software as opposed to CSG geometry where manipulation of the shapes is less convenient. A demonstration neutronics parameter study with one geometric parameter and one material parameter has been carried out to optimise TBR for the HCLL. A maximum TBR of  $1.278 \pm 0.010$  ( $5\sigma$  confidence) was found using Gaussian process to fit the data. The highest TBR value was found for a blanket design with a lithium lead poloidal height of 0.061m and a  $^6\text{Li}$  enrichment of 100%. Current the tool allows for a wide range of geometries to be made for use in simulations. Thermal-mechanical and other constraints are not taken into account when constructing the geometries and future research will be required to identify allowable design parameters that satisfy thermal-mechanical and thermal-hydraulic requirements. The geometry create can also be used in finite element and finite volume software to simulate heat diffusion, tritium diffusion and stress. A simplified heat diffusion has been demonstrated in this paper. Maximum temperature within the different materials present in the midplane slice of the HCLL outboard equatorial blanket module were found to be similar to previous research [16]. Maximum temperatures were 816K for tungsten, 859K for lithium lead and 808K for EUROfer.

## **5. Acknowledgments**

The author would like to acknowledge the financial support of EUROfusion and EPSRC. This work has been carried out within the framework of the EUROfusion Consortium and has received funding from the Euratom research and training programme 2014-2018 under grant agreement No 633053. The views and opinions expressed herein do not necessarily reflect those of the European Commission. This work has also been part-funded by the RCUK Energy Programme [grant number EP/I501045]. The author would also like to thank the HCLL, HCPB, DCLL and WCLL breeder blanket design teams.

## 6. References

- [1] J. Riegel, W. Mayer, and Y. van Havre. Freecad version 0.17. <http://freecadweb.org/>, 2001–2018.
- [2] A. Ribes and C. Caremoli. Salome platform component model for numerical simulation. *COMPSAC 07: Proceeding of the 31st Annual International Computer Software and Applications Conference*, pages pages 553–564, 2007.
- [3] T. Paviot. PythonOCC - 3D CAD for python. <http://www.pythonocc.org/>, 2015–2018.
- [4] ISO-10303-21 v214. Industrial automation systems and integration – Product data representation and exchange – Part 21: Implementation methods: Clear text encoding of the exchange structure. Standard, International Organization for Standardization, March 2016.
- [5] P. Wilson, T. Tautgesb, and J. Kraftcheck et al. Acceleration Techniques for Direct Use of CAD-based Geometries in Monte Carlo Radiation Transport. *American Nuclear Society*, 2009.
- [6] J. Leppänen, M. Pusa, and T. Viitanen et al. The Serpent Monte Carlo code: Status, development and applications in 2013. *Ann. Nucl. Energy*, 82:142 – 150, 2015.
- [7] J. Shimwell. Breeder Blanket Model Maker. DOI:<https://doi.org/10.5281/zenodo.1421059>, 2018.
- [8] P. Pereslavytsev, U. Fischer, and F. Hernandez et al. Neutronic analyses for the optimization of the advanced HCPB breeder blanket design for DEMO. *Fusion Engineering and Design*, 2017.
- [9] J.C. Jaboulay, G. Aielloa, and J. Auberta et al. Nuclear analysis of the HCLL blanket for the European DEMO. *Fusion Engineering and Design*, 2017.
- [10] A. Del Nevo, E. Martellic, and P. Agostinia et al. WCLL breeding blanket design and integration for DEMO 2015: status and perspectives. *Fusion Engineering and Design*, 2017.
- [11] I. Palermo, G. Veredas, and J.M. Gmez-Ros et al. Neutronic design studies of a conceptual DCLL fusion reactor for a DEMO and a commercial power plant. *Nuclear fusion*, 2017.
- [12] P. Pereslavytsev, P. Lu, U. Fischer. Generation of the MCNP model that serves as a common basis for the integration of the different blanket concepts. EFDA D 2M7GA5 V.1.0, 2013.
- [13] L. Lu, Y. Qiu, and U. Fischer et al. Improved solid decomposition algorithms for the CAD-to-MC conversion tool McCad. *Fusion Engineering and Design*, 2017.
- [14] Y. Wu, J. Song, and H. Zheng et al. CAD-based Monte Carlo program for integrated simulation of nuclear system SuperMC. *Annals of Nuclear Energy*, 2015.
- [15] J. Shimwell, L. Lu, and Y. Qiu et al. Automated parametric neutronics analysis of the Helium Cooled Pebble Bed breeder blanket with Be12Ti. *Fusion Engineering and Design*, 2017.
- [16] J. Aubert, G. Aiello, and G. Bongiovi et al. Design Description Document (DDD) 2016 for HCLL. DEN/DANS/DM2S/SEMT/BCCR/RT/17-027/A, 2017.
- [17] J. Peyraud. Optimization of the horizontal stiffening plates channels layout design for the Advanced-Plus concept of the DEMO HCLL Breeding Blanket. DEN/DANS/DM2S/SEMT/BCCR/NT/17-013/A, 2017.
- [18] J. Halton. Radical-inverse quasi-random point sequence. *Communications of the ACM*, 7:701–702, 1964.
- [19] IAEA. FENDL-3.1d: Fusion Evaluated Nuclear Data Library Ver.3.1d. <https://www-nds.iaea.org/fendl/>, 2018.
- [20] U. Fischer. EFDA D 2MM3A6 v1.0 - Material compositions for PPPT neutronics and activation analyses. <https://idm.euro-fusion.org/?uid=2MM3A6>, 2017.
- [21] C. Fausser et al. Tokamak D-T neutron source models for different plasma physics confinement modes. *Fusion Engineering and Design*, 2012.
- [22] U. Fischer. EFDA D 2L8TR9 v1.6 - PMI-3.3-T014-D001 - Guidelines for neutronic analyses. <https://idm.euro-fusion.org/?uid=2L8TR9>, 2017.
- [23] J. Jordanova, U. Fischer, and P. Pereslavytsev et al. Parametric neutronic analysis of HCLL blanket for DEMO fusion reactor utilizing vacuum vessel ITER FDR design. *Fusion Engineering and Design*, 2006.
- [24] C. Bowman. Inference Tools. DOI:<https://doi.org/10.5281/zenodo.1423552>, 2018.
- [25] CSimSoft. Trelis version 16.5. <https://www.csimsoft.com/>, 2018.
- [26] C. Richardson and G.N. Wells. High performance multi-physics simulations with FEniCS/DOLFIN. 5 2016. doi: 10.6084/m9.figshare.3406582.v3. URL [https://figshare.com/articles/High\\_performance\\_multi-physics\\_simulations\\_with\\_FEniCS\\_DOLFIN/3406582](https://figshare.com/articles/High_performance_multi-physics_simulations_with_FEniCS_DOLFIN/3406582).
- [27] J. Aubert, G. Aiello, and G. Bongiovi et al. Design Description Document (DDD) 2016 for HCLL. *CEA rapport technique DEN*, 2016.
- [28] J. Jordanova, U. Fischer, and P. Pereslavytsev et al. Evaluation of nuclear heating, tritium breeding and shielding efficiency of the demo hcll breeder blanket. *Fusion Engineering and Design*, 2005.
- [29] S.J Zinkle and N.M Ghoniem. Operating temperature windows for fusion reactor structural materials. *Fusion Engineering and Design*, 51-52:55 – 71, 2000. ISSN 0920-3796. doi: [https://doi.org/10.1016/S0920-3796\(00\)00320-3](https://doi.org/10.1016/S0920-3796(00)00320-3). URL <http://www.sciencedirect.com/science/article/pii/S0920379600003203>.